

Tropical Atlantic Cyclogenesis Coming from West African Mesoscale Convective Systems

Yves K. Kouadio¹, Luiz A. T. Machado^{2*} and Jacques Servain³

Prepared for Submission to *Monthly Weather Review*

October 2007

¹ University of Cocody, Abidjan, UFR-SSMT, Laboratory of Atmospheric Physics, 22 BP 582 Abidjan 22, Côte d'Ivoire. *Visiting Scientist at Divisão Satélite e Sistemas Ambientais (CPTEC/INPE), Cachoeira Paulista, SP, Brazil.*

² Centro de Previsão de Tempo e Estudos Climáticos CPTEC/INPE, Rodovia Pres. Dutra, km 40, Cachoeira Paulista, SP, Brazil.

³ Institut de Recherche pour le Développement (IRD-UR182), *Visiting Scientist at Fundação Cearense de Meteorologia e Recursos Hídricos (FUNCEME), Av. Rui Barbosa 1246, Fortaleza, CE, Brazil.*

* Corresponding author address: Luiz A. T. Machado, Centro de Previsão de Tempo e Estudos Climáticos (CPTEC/INPE), Rodovia Pres. Dutra, km 40 – 12630 000, Cachoeira Paulista - SP Brazil.
e-mail: machado@cptec.inpe.br.

Abstract

We investigate the possibility that hurricanes (H) spreading into the tropical Atlantic are originally connected with mesoscale convective systems (MCSs) previously generated on the West African continent. The analysis is carried out over 2004 and 2005, during which we find ten cases (six in 2004, four in 2005, all during July-August-September) for which such a connection can be made. For each one of the selected cases a backward methodology is performed using both subjective and objective analyses. This methodology is summarized as follows: starting from the date and position of the studied H when it is primarily catalogued as a tropical depression, we look backward at a possible easterly wave which may be the physical bond between the H initiation and an MCS dissipation in the ocean off the African coast. In this subjective step we use the wave signature from the 700 hPa vorticity at a 6-hour frequency given by the reanalysis of the NCEP, as well as the MCS dataset provided by the MSG-7 images. Having associated the easterly wave with a sufficiently consequential MCS in terms of intensity and lifespan, we proceed, in a second step, to an objective backward analysis to go up to the time until the origin (date and position) of this MCS. In this second step we adapt a recent tracking methodology (FORTRACC) to individually track each MCS at a 30-minute frequency by using a dynamical threshold temperature. We find that practically all the selected cases (9 out of 10) originate from a roughly limited area over West Africa. Mostly of MCS-H cases studied, shown an increase in the relative vorticity after MCS dissipation. As another important result, such connection between these MCSs which originate in West Africa and the occurrences of hurricanes takes place when a dipole in the sea surface temperature (SST) anomaly is observed between the Main Development Region (MDR) of the hurricanes (positive SST anomaly), and the equatorial tongue in the Gulf of Guinea (negative SST anomaly).

Key words: *Hurricanes, Mesoscale Convective Systems, Tropical Atlantic, SST dipole*

1. Introduction

The tropical North Atlantic is a basin among the world's oceans where cyclonic activity is the most intense and presents a substantial interannual and interdecadal variability (Goldenberg et al., 2001), depending directly on atmospheric and oceanic conditions. In this region cyclonic activity originates mainly from an intensification of the African easterly waves that propagate from West Africa towards the tropical North Atlantic basin and the Caribbean Sea (Shapiro, 1986; Goldenberg and Shapiro, 1996). These waves, which have a 3-to-4 day lifespan (Burpee, 1974), are responsible for about 60% of tropical storms and minor hurricanes, and 85% of hurricanes of strong intensity (Avila and Pash, 1992, 1995; Landsea, 1993). A few studies (Avila, 1991; Avila and Pasch, 1992; Molinari et al., 2000) even suggest that some tropical cyclones occurring in the eastern Pacific can develop in association with easterly waves which are initially generated in Africa, and then propagate across the tropical Atlantic and Central America.

Upstream in their propagation across the ocean, these easterly waves are themselves generally associated to mesoscale convective systems that cross the center Sahel region ranging between 8°N-18°N and 10°W-17°E and dissipate in the tropical Atlantic Ocean towards 20°W (Payne and McGarry, 1977; Simpson et al., 1997; Mathon et al., 2002a,b). Cotton and Anthes (1989) describe MCSs as deep convective systems that are considerably larger than individual thunderstorms and that are often marked by an extensive middle to upper tropospheric stratiform anvil. Some of these long-lived MCSs (1-to-4 day lifespans) could generate midlevel mesoscale vortices that take place in the stratiform region of the system after the anvil debris has dissipated (Bartels and Maddox, 1991).

In a recent study, Saïdou and Sauvageot (2005) described the cyclogenesis of hurricane Cindy (1999) in the tropical North Atlantic as resulting from a space-time conjunction between an early MCS observed off Africa and subsequent easterly wave propagation over warm sea

surface conditions. The goal of the present paper is to go further in the understanding of the relationship between the following four elements in the tropical Atlantic: (i) MCSs initiated over Africa, (ii) easterly wave propagations over the ocean, (iii) abnormal ocean surface conditions and (iv) occurrences of hurricanes.

Our analysis is based on various datasets covering the years 2004 and 2005. The hurricane data is provided by the National Hurricane Center (NHC), while atmospheric dynamic circulation features (at 700 and 1000 hPa) are extracted from the National Center for Environmental Prediction - National Center for Atmospheric Research (NCEP-NCAR) reanalysis. An original achievement for individual tracking of MCSs using Meteosat images during the two years 2004-2005 furnishes the core of this study. Oceanic surface conditions during the study period are given by sea surface temperature (SST) climatology (Reynolds et al., 2002).

The next section presents the dataset used in our analysis. We focus especially on the process developed to access to original database of MCS trajectories. Such processing allows a very precise follow-up with high frequency sampling (30-minute) of each MCS trajectory during its lifespan over the continent and the ocean. The research of occurrences of quasi simultaneity between the onset of a tropical cyclone (that later lines up in the hurricane (H) category), and the dissipation over the ocean of an MCS having been generated on the African continent, represents the midpoint of our analysis. Such events (six in 2004, four in 2005) that answer the criteria of quasi simultaneity are analyzed and described in the third section, as well as their relationship with the regional atmospheric circulation. The fourth section illustrates oceanic surface conditions which were concomitant with the selected events. A summary and conclusion appear on the last section.

2. Data and method

A classification of the intensity of the tropical cyclones is prescribed by the NHC (Landsea and Gray, 1992). Three classes are defined, from the weakest to the strongest intensity: tropical depression (TD), tropical storm (TS) and hurricane (H). Figure 1 shows the initiation coordinates for the three classes of all tropical cyclones that were observed during the years 2004 and 2005. Sixteen tropical cyclones occurred in 2004, of which nine initiated inside a zonal band limited by 15°N and 10°N, and the other seven originated at north of 22°N. Among these sixteen tropical cyclones, only one remained classified as class TD, six turned up class TS, and nine reached the H class. Among the nine H, seven hurricanes initiated inside the band 15°N-10°N: two in the vicinity of the West Indies, the five others at southwest of the Azores Islands, *i.e.* not too far from Africa. In 2005 (to date, the hottest year in the lasts two centuries; WMO, 2005), the number of tropical cyclones reached 31, *i.e.* almost double the number observed during the previous year. The repartitions of these 31 cases, according to the three classes and the initiation coordinates, are somewhat different from those for the previous year. The three classes are better distributed in space within the northern tropical basin and the West Indies region (*e.g.* there is not a concentration of H in the southwest of the Azores, as seen in 2004). Note that in 2005, 13 tropical storms out of a total of 31 (more than 40%) reached class H (including the dramatic hurricane Katrina which devastated New Orleans in August; NOAA Magazine, 2005)

MCSs are largely identified over the world's oceans by satellite images (Houze, 1977; Velasco and Fritsch, 1987; Machado and Rossow, 1993; Mathon et al., 2002a). In this study we use the digital images from the Meteosat-7 satellite over the region 25°N-25°S and 44°W-20°E, during the two periods June-to-December for 2004 and 2005. This dataset is part of the global database archived at *Centro de Previsão do Tempo e Estudos Climáticos* of the *Instituto Nacional de Pesquisas Espaciais* (CPTEC/INPE) in Brazil, available according to a 30-minute time step

and 5 km x 5 km spatial resolution (at the subsatellite point) in the infra-red channel. The June-to-December period largely covers the West African rainy season (basically from June to September) and seasonal cyclonic activity in the tropical North Atlantic (generally starting in July and ending in November). Mathon et al. (2002a) noted that these Meteosat images are useful for cloud system characterization and classification mainly in West and Central Africa, where convection is well defined on a very large scale.

The atmospheric variables are extracted from the NCEP-NCAR reanalysis dataset during the period 2004-2005. Wind data are reported on a $2.5^\circ \times 2.5^\circ$ grid every 6 hours (00:00, 06:00, 12:00 and 18:00 UT), in 17 pressure levels from 1000 hPa to 10 hPa. Because we focus on synoptic disturbances propagating in the northern Atlantic and linked to tropical cyclones, we mainly consider streamlines and relative vorticity at 700 hPa (Molinari et al., 2000).

The sea surface conditions are documented here for both years 2004 and 2005 using the Reynolds weekly SST climatology (Reynolds et al., 2002) extracted from <http://iridl-ldo.columbia.edu/>. These data are reported on a $1^\circ \times 1^\circ$ grid.

During its lifespan (generally from 1-to-4 days), an MCS can move, change, grow, decrease, split or merge in one or more systems. It is thus necessary, if one wants to correctly follow in space each event during its lifespan, to use a method which is able to adapt to successive characteristic changes of the MCS. We use here a tracking convective cluster model (FORTRACC) developed and now operational at CPTEC/INPE (Vila et al., 2007). This model takes advantage of the results of former studies such as that done by Machado and Rossow (1993), Machado et al. (1993), Machado et al. (1998), Mathon and Laurent (2001), and Machado and Laurent (2004). The FORTRACC technique is an objective method using images from geostationary satellites to individually document the physical characteristics of each MCS at each

time step during its lifespan. The main steps of this software are: (i) cloud cluster detection based on a threshold of the brightness temperature at the top of the cloud, (ii) evaluation of morphology and radiative parameters for each MCS detected in the previous step, (iii) space and time tracking for each MCS based on overlapping areas between successive images according to the 30-minute time resolution, and (iv) life cycle building and synthetic image generation.

In its basic version (Vila et al., 2007) FORTRACC uses two fixed threshold temperatures: 235 K to define the whole MCS, and 210 K to identify the areas of more intense convection embedded in this MCS. These threshold temperatures have been specified from previous works in Africa (Mathon and Laurent, 2001; and Machado et al., 1993) and in Amazonia (Machado and Laurent, 2004). In fact, the characteristics of the MCS are strongly modulated by the diurnal cycle over the continent and the ocean (*e.g.* Machado et al., 1993). For instance, when a fixed threshold is considered, there is an undervaluation of the brightness temperature over the ocean at the beginning of day. That supposes a loss of information for tracking the MCSs. Thus, it is interesting to modulate the threshold temperature daily to better follow the MCSs throughout their lifetimes, including over the ocean. We thus defined a threshold temperature following the diurnal cycle according to Morel and Senesi (2002) that showed that this method correctly discriminates 80% of MCSs in Europe. This threshold temperature is hereafter noted “dynamic temperature” in comparison with the fixed threshold temperature used in the basic version of FORTRACC. The definition of this dynamic temperature is developed in Annex 1.

During the dissipation phase of the MCS, the brightness temperature at the top of clouds increases rapidly. That makes it very difficult to follow this convective system, even while using a dynamic threshold temperature. Due to a weaker convection on the ocean, such a system generally fragments in small stratiform clouds which persist and propagate westward embedding in one of the numerous easterly wave trajectories. It thus becomes possible to continue to follow

the initial perturbation event while analyzing the signature of the associated easterly wave. These waves are generally detected from the streamfunction and relative vorticity of the wind field at 700 hPa (Berry and Thorncroft, 2005). Streamfunction has the advantage of eliminating the divergent flow. Note that many easterly waves cross the West African coast, and their number is not directly related to the number of tropical storms (Frank, 1975).

3. Tracking the MCSs and their relationship with tropical cyclogenesis

1034 long-lived MCSs (lifespan > 10 hours) initiated in West Africa from June to December in 2004 (512 MCSs) and 2005 (522 MCSs). All these MCSs initiated north of 5°N , of which 69% were between 5°N and 10°N , and only 18% between 10°N and 20°N . The remaining 13% was observed northward of 20°N . The great majority (94% of the total number) dissipated on the continent and did not reach the ocean. The remaining 6%, *i.e.* a total of 62 MCSs, dissipated over the ocean, mostly between the West African coast and 20°W .

The research of occurrences with quasi-simultaneity of time between the onset of a tropical cyclone (reaching class H) and a MCS generated over the African continent is performed as follows. We start the process with a subjective analysis from the coordinates (date and position initiation) of each one of the hurricanes observed during 2004-2005. Figure 2 illustrates one example related to hurricane “Frances” (August 2004). The top panel shows the 700 hPa streamfunction on 25 August 2004 (00:00 UT), *i.e.* the day when Frances (marked “F”) was primarily classified as TD only. From this date, and from the area of initiation of this tropical cyclone, we look at synchronous and backward streamfunction patterns at a 6-hour frequency to seek a possible signature of an easterly wave. If succeeding in such research (as was the case for Frances, for instance), we continue the process backward (Figs. 2b,c,d,e) until we find when and where the easterly waves left the West African coast (*e.g.* about 15°W in the current example). At

this point of the subjective analysis, we then look at the MCSs which could be present within this area in the same time (*i.e.* within the same 6-hour time step). From all the possible concomitant MCSs, we select one whose size is greater than 5000 km² (Mathon et al., 2002a), whose lifespan is longer than 10 hours, and that displaces roughly westward, *i.e.* in the direction of the easterly wave previously analyzed (Mathon et al., 2002b). The identified MCS (marked on Fig. 2e in the current example by its center of mass and its circle of activity) is thus located ahead of the easterly wave disturbance trough. Then, using the FORTRACC technique, and starting from the date of the dissipation position of this selected MCS, we achieve the process by a backward objective analysis along the MCS track until the date and position of its initiation over the African continent. The entire process, combining diagnostic subjective and analytic objective analyses, thus allows the identification of a MCS generated over the African continent. Such an MCS is supposed to be the very early event responsible (a few days before) for the current hurricane. This process was applied to each one of the 22 hurricanes observed in 2004-2005. Six events in 2004 (Charley, Frances, Ivan, Jeanne, Karl and Lisa) and four events in 2005 (Dennis, Emily, Irene and Maria) succeeded the process and were finally selected (see Table 1). The lack of the last Meteosat images in the case of Emily (2005), involves a bad determination of the related MCS dissipation day. Based in the available images, the MCS related to Emily dissipated some time between July 07 at 7:30 UT and 10:30 UT. For reference we defined the dissipation day as being the time of the last available image. In the case of Danielle (2004), the bad quality of the satellite images from August 11 at 02:30 UT to August 12 at 16:30 UT caused a lack of data and the MCS could not be tracked. The others tropical cyclones did not fulfill our selection criteria. All the ten selected MCSs initiated during the July-September period when a midlevel African easterly jet is intensified.

Following the idea of the backward process previously described, and complementing the example shown in Figure 2, the next four figures (Figs. 3, 4, 5, and 6) illustrate some points of our analysis, starting from the hurricane episodes and going back in time until the MCS initiations.

700 hPa unfiltered relative vorticity is used to describe the easterly waves. Figure 3 shows the Hovmöller space-time diagrams for this variable averaged between 5°N and 15°N for the 3-month period J-A-S of 2004 (top) and 2005 (bottom). Many easterly waves propagate along the 10°E to 65°W longitudes at an average speed of about 10 m s^{-1} , in agreement with the literature (Burpee, 1974). The ten previously selected events, indicated by hurricane names (6 in 2004, 4 in 2005), are schematically represented. Centers of mass of the MCSs at the date of their dissipation phase (dots) and the hurricane initiation coordinates (stars) are connected by a dashed line that always follows an easterly wave trajectory. In the case of Emily (2005), the MCS probably dissipated a few hours later than previously mentioned, and would be in the band of higher relative vorticity. There is not, however, an apparent relationship between the occurrence of these events and a stronger intensity of the waves. This is right, for instance, for the two events associated with Ivan (2004) and Maria (2005): the easterly wave linked to Ivan is of weak intensity ($< 0.2 \cdot 10^{-5} \text{ s}^{-1}$), while the easterly wave linked to Maria is of very strong intensity ($> 2.2 \cdot 10^{-5} \text{ s}^{-1}$). These two cases are somewhat different in the sense that the time lag between the dates of the MCS dissipation and H initiation varies from about 2 days, in the case of Ivan, to about 5 days in the case of Maria. The distances between the coordinates of the MCS dissipations and those of the H initiations are also different (1545 km for Ivan, 3752 km for Maria). Time lags and distances are compatible with a common “virtual” celerity of the signal between the two phenomena for each case (9.3 m s^{-1} for both events). In fact, when averaged over the ten selected cases in 2004 and 2005 (see Table 1), such celerity is $9.7 (\pm 1.0) \text{ m s}^{-1}$, *i.e.* a celerity fully

compatible with the easterly wave propagation (Burpee, 1974). The distance between coordinates of the MCS dissipations and the tropical cyclone initiations lies between 1000 km (~ 2 days) and 4800 km (~ 5 days). These distances are shorter on average in 2004 (2800 km) than in 2005 (3100 km).

Figure 4 shows an example for 2004 (Ivan) and 2005 (Maria) of the 700 hPa unfiltered relative vorticity on the MCS dissipation day, the day before the MCS dissipation and up to the day of the hurricane initiation. This Figure also shows the position of the MCS dissipation and the hurricane initiation. The 700 hPa relative vorticity increases westward one day after the MCS dissipation with a well defined relative vorticity high value of $2.0 \cdot 10^{-5} \text{ s}^{-1}$ at about $11^{\circ}\text{N}-0^{\circ}\text{W}$ during 2004 and of $2.5 \cdot 10^{-5} \text{ s}^{-1}$ at about $11^{\circ}\text{N}-20^{\circ}\text{W}$ during 2005, while it reaches a value of almost $1.0 \cdot 10^{-5} \text{ s}^{-1}$ the day of the dissipation in the vicinity of the MCS dissipation for the two years. The increase in the vorticity after the MCS dissipation can be related to the westward advection of the fragmented stratiform parts of the long-lived convective systems as suggested by Bartels and Maddox (1991). The fragmented stratiform clouds weaken the flow and the vertical shear of the zonal wind and increase the horizontal and vertical moisture gradients (Bartels and Maddox, 1991; Saidou and Sauvageot, 1995). Therefore, the characteristics described by the MCS dissipation and the subsequent synoptic condition of fragmented stratiform clouds can increase the cyclonic vorticity and can be explained by the increase in the stretching term of the vorticity equation. This behavior could contribute to intensifying the easterly wave and help the development of the tropical cyclone as suggested by Houze (2004), by triggering the first convective burst. Observing the Hovmöller diagram in Figure 3, in the great majority of the cases the increase in relative vorticity after the MCS dissipation phase can be noted. It is also true for Emily if we consider that the dissipation happened after the last available image, as already discussed. Figure 5 illustrates the geographical expansions of the ten selected MCS trajectories

that crossed or reached the West African coast. The lifespans vary from 22.5 hours (Jeanne) to 87.5 hours (Dennis) (see Table 1). To simplify, we assume a disc surface proportional to the real area. A possibility that an MCS can merge or split is taken into account. The area grows especially during the period when the MCSs remain over the continent, thus corresponding to a strong convection and upper air wind divergence (Machado and Laurent, 2004).

Finally, at the ending point of our atmospheric analysis, but at the very early point of the analytical process, Figure 6 shows the initiation coordinates for the ten selected MCSs. Except for one event (see after), these coordinates are distributed inside the same relatively limited continental domain: 5°N - 11°N , 8°W - 2.5°W . Only the MCS associated with hurricane Dennis (June 2005) initiated around 6°E , *i.e.* at east of that region. The lifespan of this last MCS was exceptionally long (87.5 hours); definitely longer than the average of the 9 others events (33 hours).

4. Surface ocean conditions in 2004 and 2005

The relationship identified in the previous section through our multi-analysis technique between MCS dissipations and tropical cyclone initiations could have been related to specific patterns in ocean surface conditions. Investigating this hypothesis, we used the weekly SST provided by Reynolds et al. (2002). The two SST composite patterns from 20°N to 10°S , formed by averaging the five¹ (four) weekly SST fields closest to the six (four) occurrences linking an MCS to a hurricane during 2004 (2005) are shown in Figure 7. The signatures of the trajectories between the MCS dissipations and the H initiations (as previously illustrated on Fig. 3) are superimposed on the SST patterns. It is not surprising to note that all the selected events are born

¹ We used only five SST anomaly patterns in 2004 because the events related to hurricanes Karl and Lisa occurred within the same week in September

and grow inside the width 10°N-20°N where the SST is the warmest ($> 27^{\circ}\text{C}$). That region, called the Main Development Region (MDR), is currently known as the region of frequent hurricane development (Goldenberg and Shapiro, 1996). The warm SST conditions are somewhat more intense in 2005 vs. 2004 in the vicinity of the African continent. Conversely, the equatorial tongue is colder and expands more westward in 2005 than in 2004. That induces a more pronounced meridional gradient between warm and cold regions in the 2005 composite vs. the 2004 composite. This result is strengthened by Figure 8 where we plotted the nine weekly SST anomaly patterns related to each one of the events identified in this study. The SST anomaly patterns are computed through a deviation from an SST weekly climatology performed in the years 1971-2000 (Reynolds et al., 20002). Appearing clearly for most of the cases, we observe abnormal warm conditions ($> 1^{\circ}\text{C}$) in the region of hurricane formation, and negative SST anomaly in the region of MCS dissipations. Furthermore, especially for all four events in 2005, the Gulf of Guinea was colder than normal, particularly during the two first events (Denis and Emily in early July). That was also the case, but with a weaker signal, for Charley and Frances, the two first events in 2004. The SST anomaly composite of all these events (right-bottom panel of Fig. 8) provides a smoothed illustration of that dipole phenomenon.

5. Summary and conclusion

The main objective of this study was to analyze a possible connection between MCSs initiated in West Africa and the cyclogenesis observed in the tropical Atlantic. The study is carried out for the years 2004 and 2005. The MCS dataset is obtained from digital satellite images of the Meteosat-7 providing the brightness temperature at the top of the clouds. The MCSs are individually tracked using an adaptation of the FORTRACC algorithm model to generate trajectories at a 30-minute frequency. In order to follow the systems over the ocean, an

innovative threshold temperature called “dynamic temperature” is defined and applied to the convective clusters. Only MCSs whose lifespan was greater than ten hours were retained after running the algorithm model.

Looking among the 22 tropical cyclones which produced hurricanes in 2004 (9 cases) and 2005 (13 cases), we identified those that could have been directly associated to one of the MCSs previously retained. Such identification is made by using a subjective-objective composite backward analysis. Six cases in 2004 and four cases in 2005 were selected. The dissipation coordinates of the ten selected MCSs are located ahead of a wave disturbance trough. The time lags and the distances between the MCS dissipations and the hurricane initiations vary from 1 to 5 days and from 1000 to 4800 km respectively. That indicates a mean “virtual” celerity of about $9.7 \pm 1.0 \text{ ms}^{-1}$, compatible with the mean speed of easterly wave propagations. Indeed, at the dissipation phase, the MCSs are not captured by the FORTRACC algorithm, although they remain active. They transform into hot clouds, and then fragment in small stratiform parts that propagate westward embedding in the easterly wave trajectory.

The analysis of each one of the ten selected cases is completed and illustrated by a set of comparisons using 700 hPa relative vorticity. An increase of cyclonic vorticity is founded at 700 hPa in the vicinity of each one of the stratiform MCS dissipation coordinates, one day after this dissipation.

Looking backwards in the time it was noted that practically all the selected MCSs originated in the same continental domain roughly spreading out from the Ivory Coast. This rather limited territory is located more to the south and more to the east than the center Sahel previously noted by various authors (see in Introduction) when they linked MCSs and (only) easterly waves propagating over the Atlantic Ocean. The present result, which links African

MCSs, easterly waves over the ocean and hurricanes, thus creates matter of very special attention in this new area.

Observed SST patterns over the tropical Atlantic indicated abnormal warm ocean conditions during the ten selected events in the MDR of the hurricanes. In the meantime, the cold equatorial tongue was colder and more expanded than normal. It seems, thus, that beyond the already known warming condition in the MDR (which remains a necessary condition to initiate hurricanes), such a strengthening in the NW-SE gradient of SST favors connecting such hurricane occurrence with an early MCS leaving West Africa a few days before. That result needs to be verified for other years, and the PIRATA moorings which are located in the region (see right-bottom panel of Fig. 8) are excellent candidates to test and monitor such a hypothesis.

This work shows the pertinence of tracking the MCSs leaving West Africa which could act on the tropical cyclogenesis of the tropical North Atlantic. This primary diagnostic study invites us to use a coupled circulation model to better understand how these various climatic elements interact. This could help in forecasting the tropical cyclones which form in the Atlantic Ocean.

Acknowledgments: This work is part of the CNPq-IRD Project "Climate of the Tropical Atlantic and Impacts on the Northeast" (CATIN), N^o CNPq Process 492690/2004-9. Y. K. K. stayed in *Centro de Previsão do Tempo e Estudos Climáticos* of the *Instituto Nacional de Pesquisas Espaciais* (CPTEC/INPE) in Brazil was supported by an IRD-EGIDE grant (2006-2007). Statistics for tropical Atlantic cyclones are obtained from the National Hurricane Center (NHC). The SST data are from Reynolds and Smith (2002). Wind data are provided from the NCEP/NCAR Reanalyses.

Annex 1

From an arbitrary selection of the available 2004-2005 MCS dataset over the ocean an analysis is performed to define the dynamic temperature which is subsequently used. The occurrence probabilities (not shown) are firstly calculated to have a cloud top brightness temperature lower than 235 K (hereafter noted T_{235}). For instance, this probability is 9.0 % at 19:00 UT and only 4.6% at 16:00 UT. Therefore the probability of 9 % at the time of maximum ocean activity is considered to define a dynamic temperature that allows the tracking of the MCSs even during suppressed diurnal cycle activity.

All the brightness temperatures less than 300 K in each image are classified in ascending order. n_t is the number of brightness temperature values lower than 300 K for each image, and

$Pb(0.09) = \frac{N}{n_t}$ is the probability equal to 9 % for a brightness temperature (T_{IR}) at the N^{th} position.

The position N is calculated by:

$$N = \text{int}(n_t * 0.09) \text{ where } \text{int} \text{ is the integer part of the product } n_t * 0.09.$$

Finally, the T_{IR} (noted hereafter T_{CC}) value is calculated at this N position for each image. This technique provides an adaptive brightness threshold temperature for each moment of the day, and thus that allows following each MCS with the best accuracy.

As seen previously, FORTRACC uses two threshold temperatures, one to define the MCS as a whole (T_{CC}), and another (lower) to define the more intense cells which can merge inside the MCS. To define a dynamic temperature (noted T_b) for this colder temperature the same

procedure was applied by considering the probability for a brightness temperature equal to 210 K (this is the usual value used for the coldest threshold).

Figure A1 shows the diurnal evolution for T_{CC} and T_b on the ocean, as well as the brightness temperature T_{235} fixed at 235 K. As already observed in previous works (Chen and Houze, 1997; Hall and Vonder Haar, 1999) the convective activity is higher at end of night and early morning. Then, T_{CC} and T_b decreases from 10:00 UT to 18:00 UT when T_{CC} becomes equal to T_{235} . The comparison between FORTRACC outputs using fixed temperature (T_{235}) and outputs using the dynamic temperature (T_{CC}) reveals (Table A1) constantly more numerous events with a larger cloud cover (higher by a factor of 1.4 the total cloud cover and by a factor of 1.3 for the total MCS number) and longer MCS trajectories for the T_{CC} case (not shown).

References

- Avila, L. A., R. J. Pash, 1991: Atlantic Tropical Systems of 1990. *Mon. Weather Rev.*, **119**, 2027–2033.
- , R. J. Pash, 1992: Atlantic Tropical Systems of 1992. *Mon. Weather Rev.*, **120**, 2688–2696.
- , R. J. Pash, 1995: Atlantic Tropical Systems of 1993. *Mon. Weather Rev.*, **123**, 887–896.
- Bartels, D. L., and R. A. Maddox, 1991: Midlevel cyclonic vortices generated by mesoscale convective systems, *Mon. Weather Rev.*, **119**, 104–118.
- Berry, G. J. and C. Thorncroft, 2005: Case study of an intense African Easterly Wave. *Mon. Weather Rev.*, **133**, 752-766.
- Burpee, R. W., 1974: Characteristics of North African Easterly Waves During the Summers of 1968 and 1969. *Jour. Atm. Sci.*, **31**, 1556-1570.
- Chen, S. S., and R. A. Houze Jr., 1997: Diurnal variation and lifecycle of deep convective systems over the tropical Pacific warm pool. *Q. J. R. Meteorol. Soc.*, **123**, 357–388.
- Cotton, W. R., and R. A. Anthes, 1989: *Storm and Cloud Dynamics*. Academic Press-Harcourt Brace Jovanovich, 880 pp.
- Frank, N. L., 1975: Atlantic Tropical Systems of 1974. *Mon. Weather Rev.*, **103**, 294–300.
- Goldenberg, S. B., C. W. Landsea, A. M. Mestas-Nun and W. M. Gray, 2001: The Recent Increase in Atlantic Hurricane Activity: Causes and Implications. *Science*, www.sciencemag.org, **293**, 474-479.
- , and L. J. Shapiro, 1996: Physical mechanisms for the association of El Niño and West African rainfall with Atlantic major hurricanes. *J. Climate*, **9**, 1169–1187.

- Hall, T. and T. H. Vonder Haar, 1999: The Diurnal Cycle of West Pacific Deep Convection and Its relation to Spatial and Temporal Variation of Tropical MCSs. *J. Atmos. Sci.*, **56**, 3401-3415.
- Houze, R. A., Jr., 1977: Structure and dynamics of a tropical squall-line system, *Mon. Weather Rev.*, **105**, 1540–1567.
- , 2004 : Mesoscale convective systems, *Rev. Geophys.*, **42**, RG4003, doi:10.1029/2004RG000150.
- Landsea, C. W, 1993: A Climatology of Intense (or Major) Atlantic Hurricanes. *Mon. Weather Rev.*, **121**, 1703-1713.
- , and W. M.Gray 1992: The strong association between western Sahelian monsoon rainfall and intense Atlantic hurricanes. *Mon. Weather Rev.*, **5**, 435-453.
- , J. P. Duvel and M. Desbois, 1993: Diurnal Variations and Modulation by Easterly Waves of the Size Distribution of Convective Cloud Clusters over West Africa and Atlantic Ocean. *Mon. Weather Rev.*, **121**, pp. 37-49.
- , R. L. Guedes and A. W. Walker, 1998, Life Cycle Variations of Mesoscale Convective Systems over the Americas. *Mon. Weather Rev.*, **126**, 1630-1654.
- , and W. B. Rossow, 1993: Structural characteristics and radiative properties of tropical cloud clusters. *Mon. Wea. Rev.*, **121**, 3234–3260.
- , and H. Laurent, 2004: The Convective System Area Expansion over Amazonia and Its Relationships with Convective System Life Duration and High-Level Wind Divergence. *Mon. Weather Rev.*, **132**, 714-725.
- Mathon, V. and H. Laurent, 2001: Life Cycle of the Sahelian Mesoscale Convective Cloud Systems. *Quart. J. Roy. Meteor. Soc.*, **127**, 377-406.

- , H. Laurent and T. Lebel, 2002a: Mesoscale Convective System Rainfall in the Sahel. *J. Climate*, **141**, 1081-1092.
- , A. Diedhiou and H. Laurent, 2002b: Relationship between easterly waves and mesoscale : *Geoph. Res. Letters*, **29**, No. 0, 10.1029/2001GL014371.
- Molinari J., D. Vollaro, S. Skubis and M. Dickinson, 2000: Origins and Mechanisms of Eastern Pacific Tropical Cyclogenesis: A Case Study. *Mon. Weather Rev.*, **128**, 125–139.
- Morel, C. and S. Senesi, 2002 : A Climatology of Mesoscale Convective Systems over Europe Using Satellite Infrared Imagery. I : Methodology. *Quart. J. Roy. Meteor. Soc.*, **128**, 1953-1992.
- NOAA Magazine, 2005: <http://www.magazine.noaa.gov/>.
- Payne, S. W., and M. M. McGarry, 1977: The relationship of satellite inferred convective activity to easterly waves over West Africa and the adjacent ocean during phase III of GATE. *Mon. Weather Rev.*, **105**, 413–420.
- Reynolds, R. W., N. A. Rayner, T. M. Smith, D. C. Stokes, and W. Wang, 2002: An improved in situ and satellite SST analysis for climate. *J. Climate*, **15**, 1609-1625.
- Saïdou and H. Sauvageot, 2005: Cyclogenesis off the African Coast: The Case of Cindy in August 1999. *Mon. Weather Rev.*, **133**, 2803-2813.
- Shapiro, L. J., 1986: The three-dimensional structure of synoptic-scale disturbances over the tropical Atlantic. *Mon. Weather Rev.*, **114**, 1876–1891.
- Simpson, J., E. Ritchie, G. J. Holland, J. Halverson and S. Stewart, 1997: Mesoscale Interactions in Tropical Cyclone Genesis. *Mon. Weather Rev.*, **125**, 2643-2661.
- Velasco, I., and J. M. Fritsch, 1987: Mesoscale convective complexes in the Americas, *J. Geophys. Res.*, **92**, 9591–9613.

Vila D. A., Machado L.A.T. and I. Velasco, 2007: Forecast and Tracking the evolution of cloud cluster (ForTraCC) using infrared imagery: Methodology and Validation. Submitted to the *Weather and Forecasting*.

WMO, 2005: *WMO statement on the status of the global climate in 2005*. WMO Report N° 998, 12 pp.

LIST OF FIGURES AND TABLE

Figure 1: Initiation coordinates of the tropical cyclones observed during the years 2004 and 2005. Every symbol is related to tropical cyclones which remained as tropical depression (TD), or turned as tropical storm (TS) or hurricane (H).

Figure 2: 700 hPa streamline ($\times 10^{-5} \text{ m}^2 \text{ s}^{-1}$) fields (contours) over the tropical North Atlantic (40°W - 10°E), plotted backwards from 25 August 2004 (a panel) at 00:00 UT to 21 August 2004 at 12:00 UT (e panel). Intermediate daily fields at 00:00 UT (b, c, and d panels) are plotted. The star (a panel) marks the coordinates of the initiation position of the hurricane Frances. Position (black cross) and intensity (black circle) of the MCS associated to Frances are marked on e panel, when the 700 hPa streamline disturbance is localized on the African coast. Wind velocity ($> 8 \text{ m s}^{-1}$) at the 700 hPa level is also plotted (dashed contour).

Figure 3: Hovmöller diagrams along 65°W - 10°E in J-A-S of 2004 (top panel) and 2005 (bottom panel) of the 700 hPa relative vorticity ($\times 10^{-5} \text{ s}^{-1}$) averaged between 5°N and 15°N . For each one of the ten selected cases (related here by H names), the hurricane initiation coordinates (black stars) and the center of mass of the associated MCS during its dissipation phase (black dots) are linked by a dashed line.

Figure 4: 700 hPa unfiltered relative vorticity for the Ivan (left) and Maria (right) cases from the MCS dissipation day at 19:00 UT (for Ivan) and 19:30 UT (for Maria) up to the day of the hurricane initiation. Only positive values larger than $0.5 \times 10^{-5} \text{ s}^{-1}$ are plotted. The contour

increment is $0.5 \times 10^{-5} \text{ s}^{-1}$. Positions of the MCS dissipations and hurricane initiations are indicated by black dots and black stars respectively.

Figure 5: Space evolutions of the ten selected MCSs which initiated over West Africa in 2004 (six panels in the top) and in 2005 (four panels on bottom). MCS displays, considered here to be quasi-circular, are plotted every 6-hour from the initiation date (dot) to the dissipation date (star). The mean trajectories, always roughly westward, are also represented. Systems that vanish by merge or split are taking account.

Figure 6: Spatial distribution of the initiation coordinates for the ten selected MCSs in 2004 (filled circles) and 2005 (filled triangles).

Figure 7: Weekly SST composites computed from the six selected events in 2004 (top) and the four selected events in 2005 (bottom). Interval contour is 0.5°C . Coordinates of the centers of mass of the MCSs at their dissipation phase (black dots) and those of the H initiations (black stars) are indicated, as well as their distances.

Figure 8: Weekly SST anomalies averaged over each period ranged between MCS dissipations and H initiations during 2004 (left) and 2005 (right). Interval contour is 0.2°C . Coordinates of MCS dissipations and H initiations are marked as in Fig. 7. The right-bottom panel (with the schematically locations of the PIRATA array) represents the average of all the other panels.

Figure A1: Threshold temperatures used to track the MCSs in the ocean. The continuous curve (T_{cc}) is the dynamical threshold temperature used to define the MCSs, and the dotted curve (T_b)

is the dynamical threshold temperature used to define the convective cells merged inside the MCSs. The fixed T_{235} is represented by a horizontal line.

Table 1: Summary information on the ten cases selected in 2004 and 2005 when hurricanes are associated to MCSs originating from the African continent. Distance (km) and time lag (day) between MCS dissipations and hurricane initiations are indicated, as well as the mean virtual velocity (m s^{-1}). MCS initiation dates and their lifespans are also given.

Table A1: Summary information on the tracking MCSs for the case of August 2004 between 44°W - 20°E ; 25°S - 25°N .

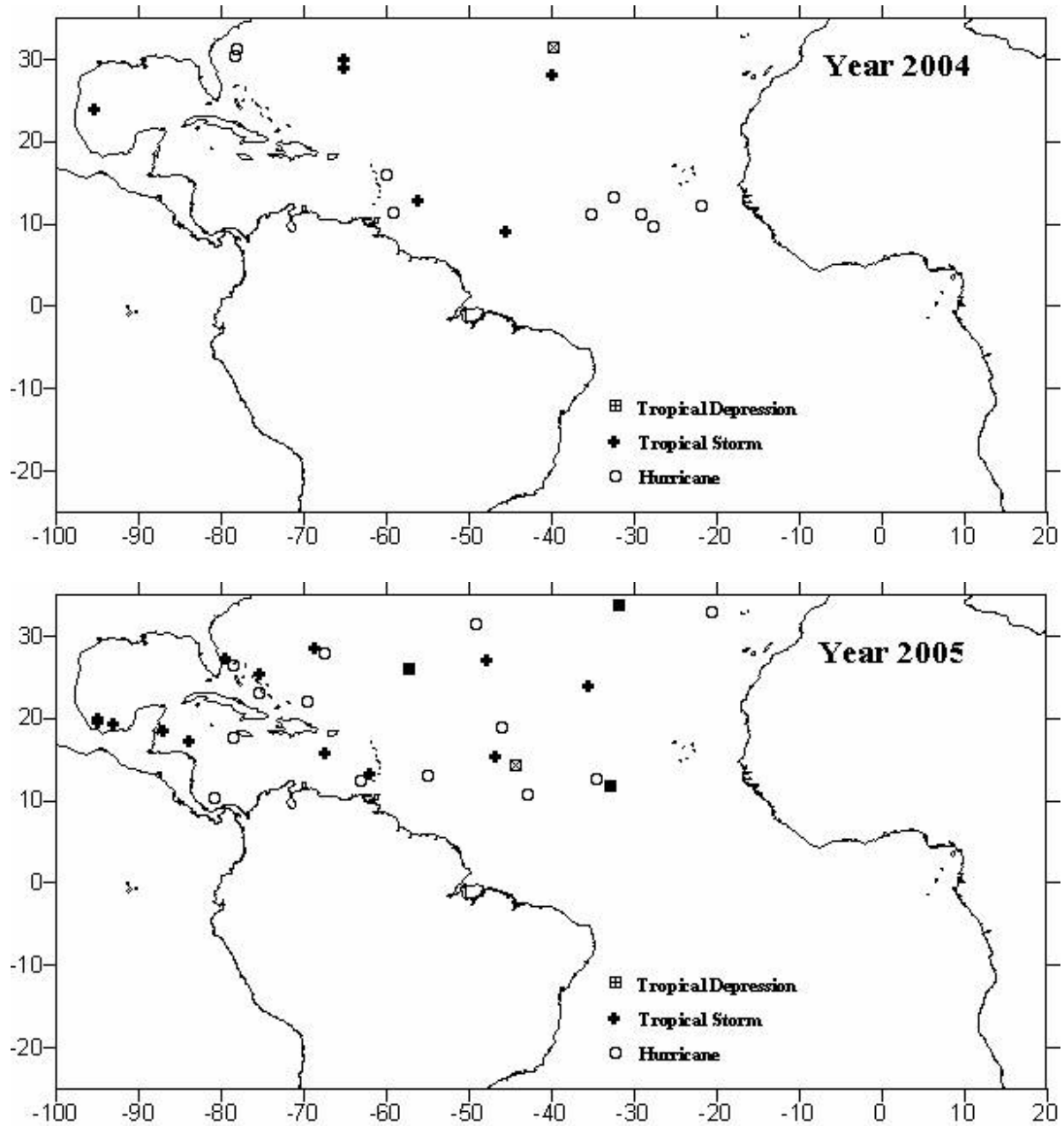


Figure 1: Initiation coordinates of the tropical cyclones observed during the years 2004 and 2005. Every symbol is related to tropical cyclones which remained as Tropical Depression (TD), or turned as Tropical Storm (TS) or Hurricane (H).

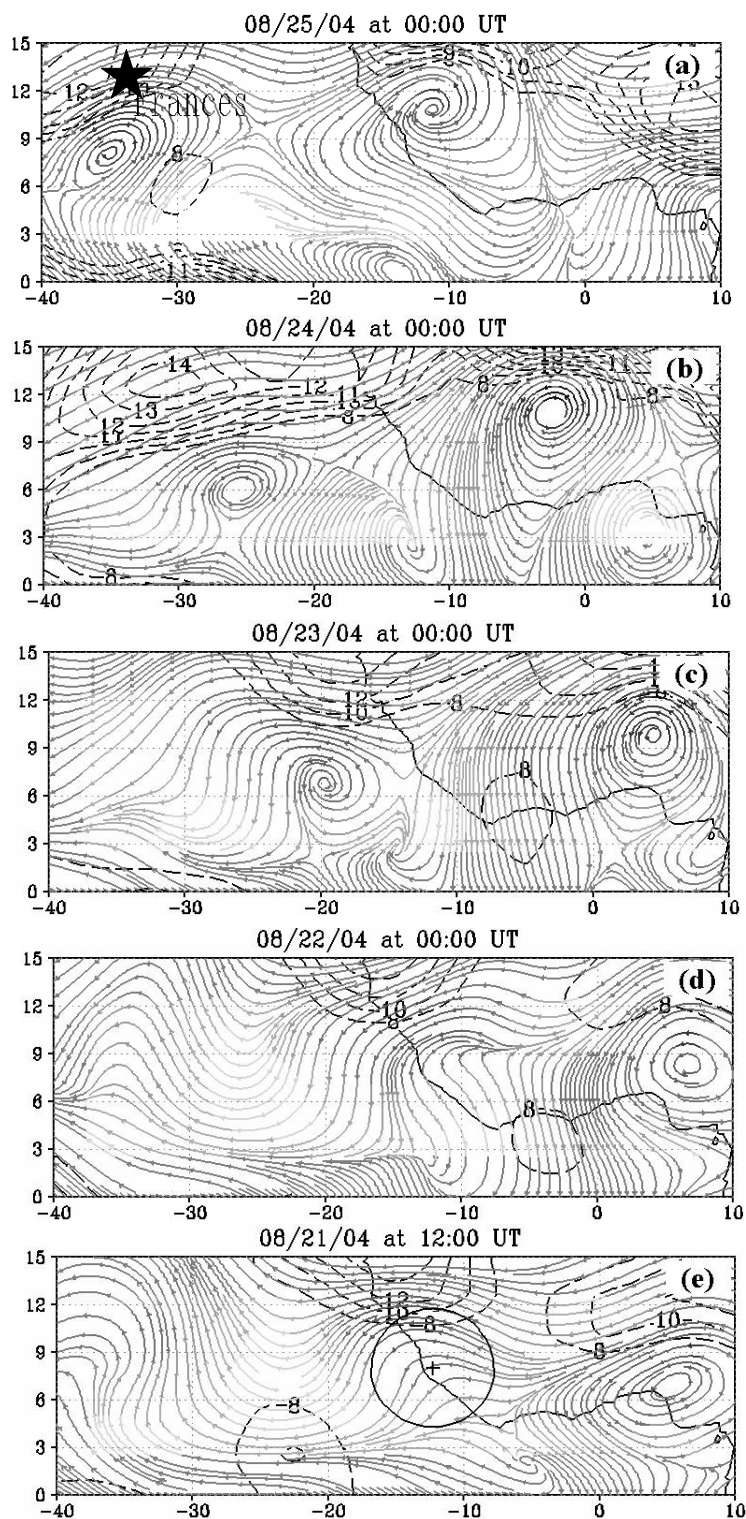


Figure 2: 700 hPa streamline ($\times 10^{-5} \text{ m}^2 \text{ s}^{-1}$) fields (contours) over the tropical North Atlantic (40°W - 10°E), plotted backwards from 25 August 2004 (a panel) at 00:00 UT to 21 August 2004 at 12:00 UT (e panel). Intermediate daily fields at 00:00 UT (b, c, and d panels) are plotted. The star (a panel) marks the coordinates of the initiation position of the hurricane Frances. Position (black cross) and intensity (black circle) of the MCS associated to Frances are marked on e panel, when the 700 hPa streamline disturbance is localized on the African coast. Wind velocity ($> 8 \text{ m s}^{-1}$) at the 700 hPa level is also plotted (dashed contour).

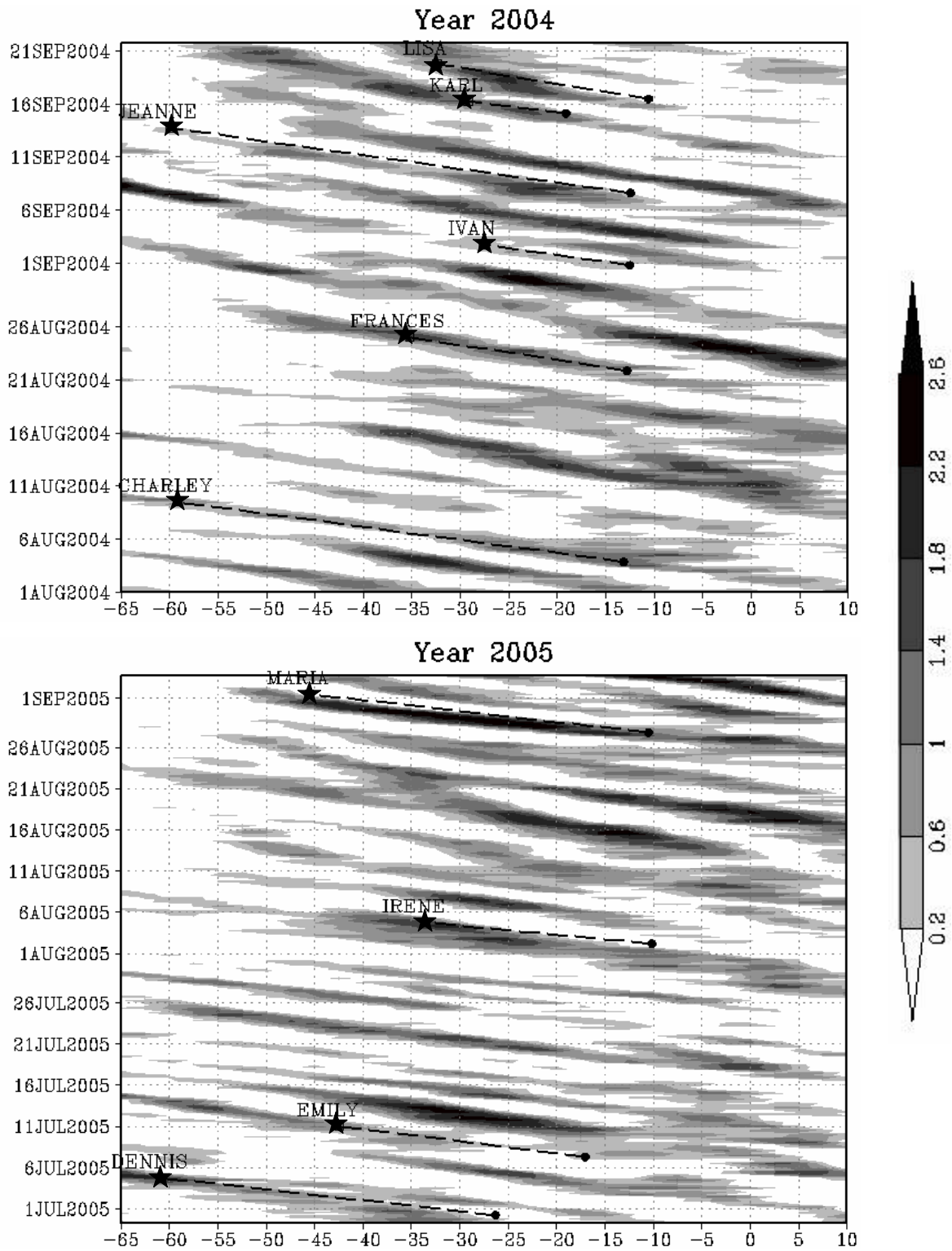


Figure 3: Hovmöller diagrams along 65°W - 10°E in J-A-S of 2004 (top panel) and 2005 (bottom panel) of the 700 hPa relative vorticity ($\times 10^{-5} \text{ s}^{-1}$) averaged between 5°N and 15°N . For each one of the ten selected cases (related here by H names), the hurricane initiation coordinates (black stars) and the center of mass of the associated MCS during its dissipation phase (black dots) are linked by a dashed line.

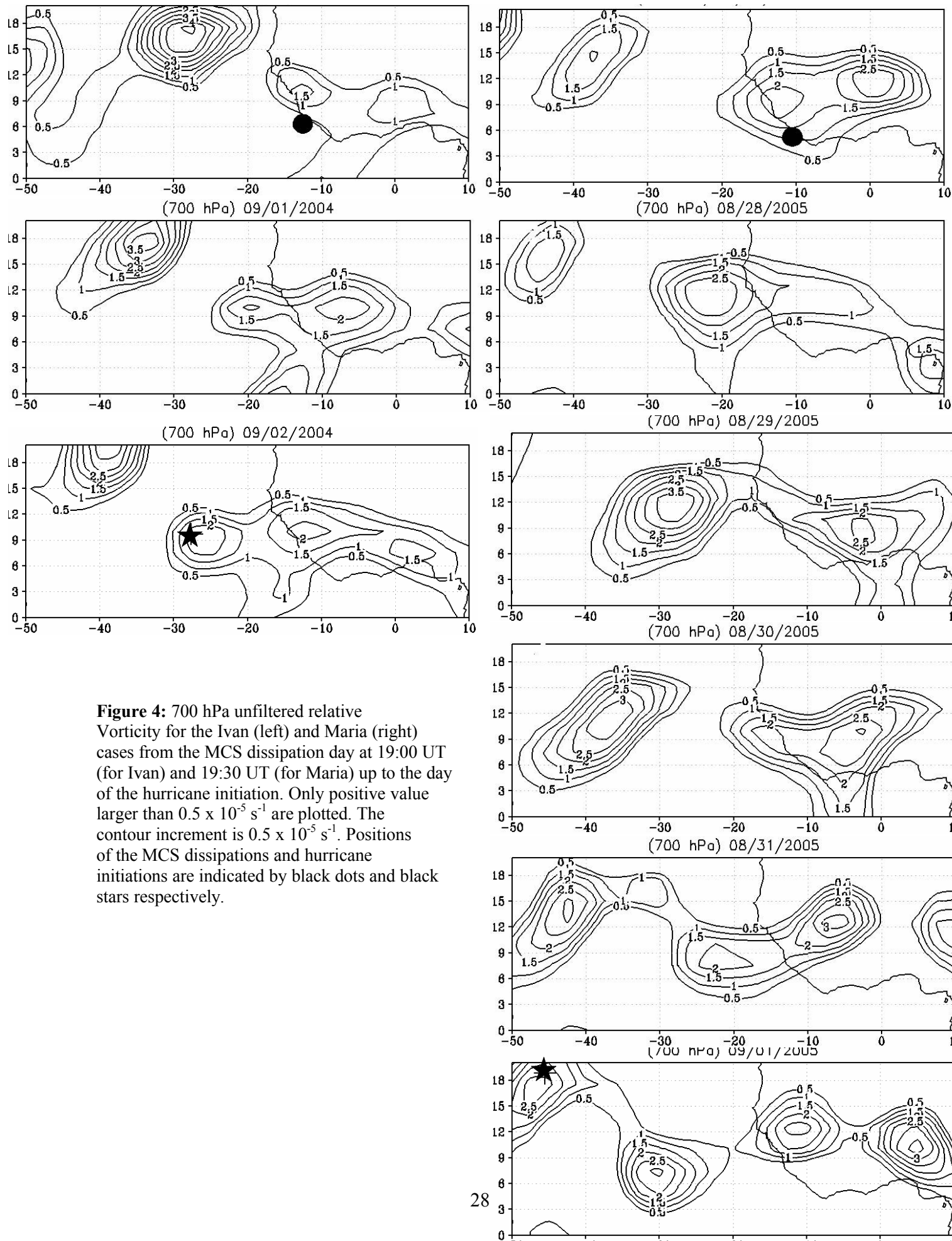


Figure 4: 700 hPa unfiltered relative Vorticity for the Ivan (left) and Maria (right) cases from the MCS dissipation day at 19:00 UT (for Ivan) and 19:30 UT (for Maria) up to the day of the hurricane initiation. Only positive value larger than $0.5 \times 10^{-5} \text{ s}^{-1}$ are plotted. The contour increment is $0.5 \times 10^{-5} \text{ s}^{-1}$. Positions of the MCS dissipations and hurricane initiations are indicated by black dots and black stars respectively.

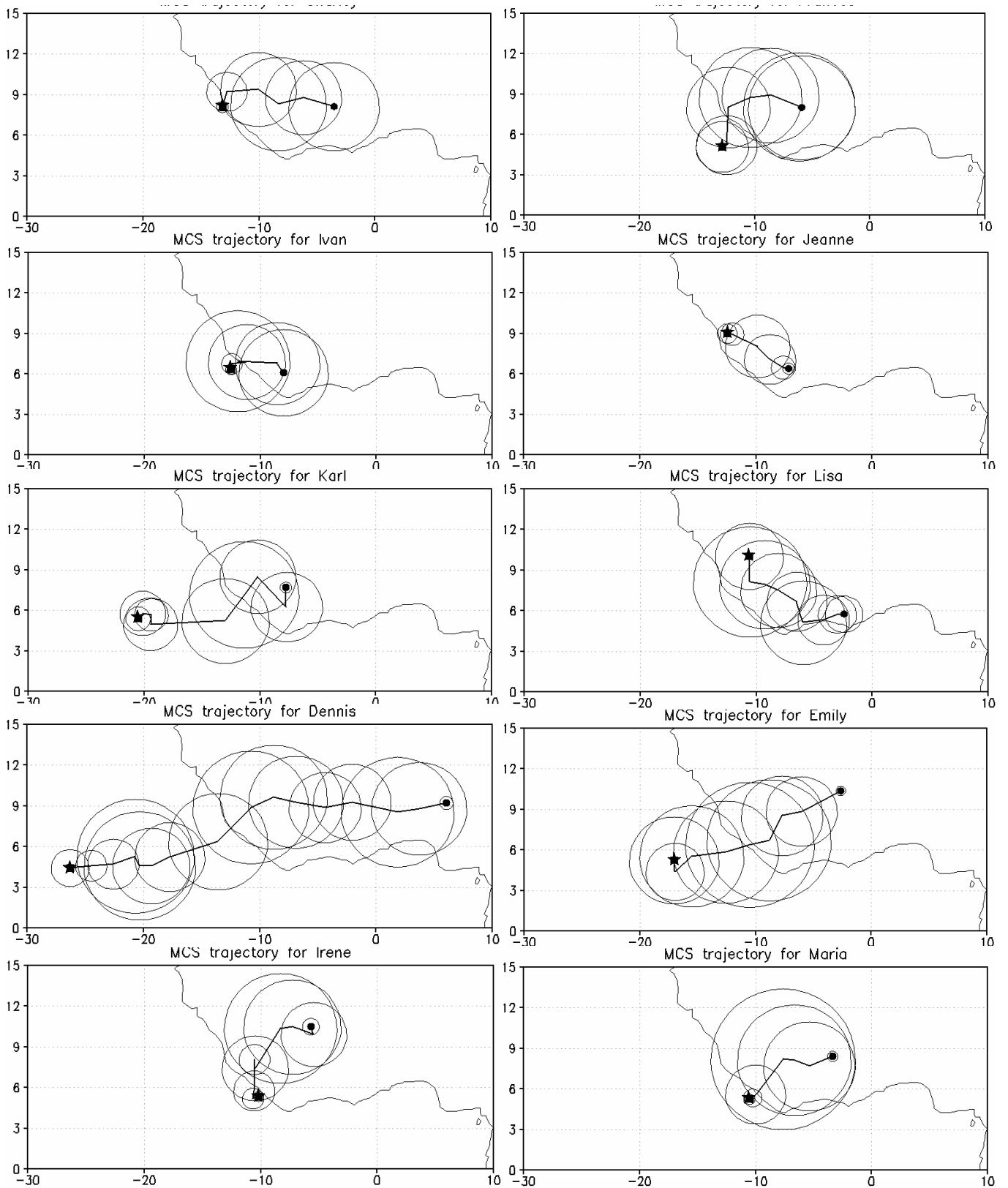


Figure 5: Space evolutions of the ten selected MCSs which initiated over West Africa in 2004 (six panels in the top) and in 2005 (four panels on bottom). MCS displays, considered here to be quasi-circular, are plotted every 6-hour from the initiation date (dot) to the dissipation date (stars). The mean trajectories, always roughly westward, are also represented. Systems that vanish by merge or split are taking account.

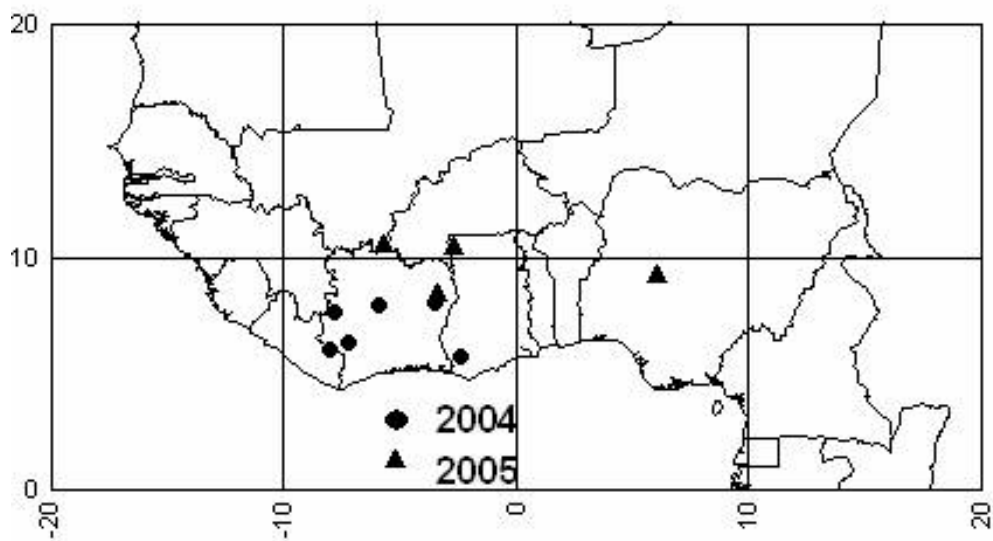


Figure 6: Spatial distribution of the initiation coordinates for the ten selected MCSs in 2004 (filled circles) and 2005 (filled triangles).

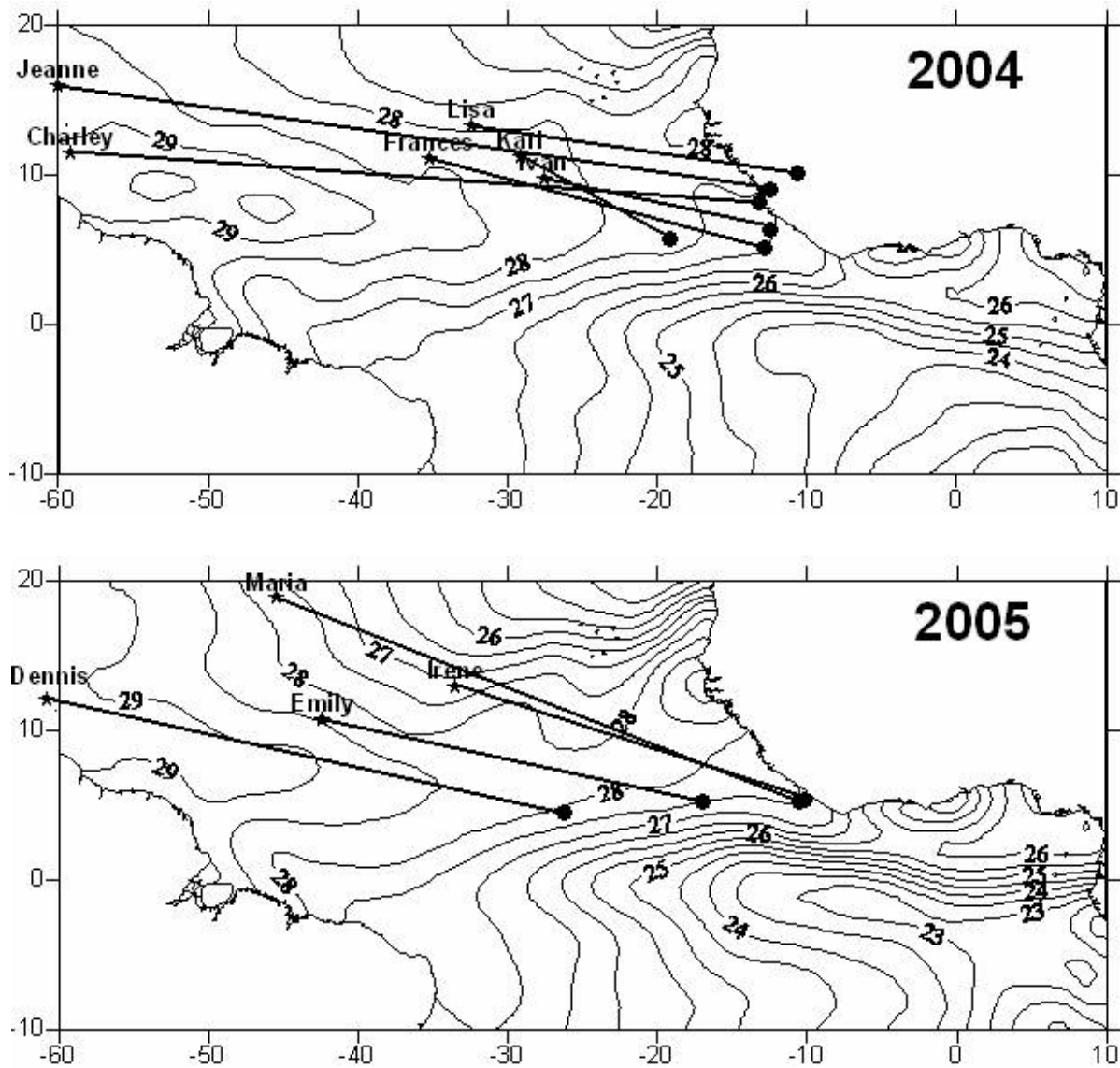


Figure 7: Weekly SST composite computed from the six selected events in 2004 (top) and the four selected events in 2005 (bottom). Interval contour is 0.5°C. Coordinates of the centres of mass of the MCSs at their dissipation phase (black dots) and those of the H initiations (black stars) are indicated, as well as their distances.

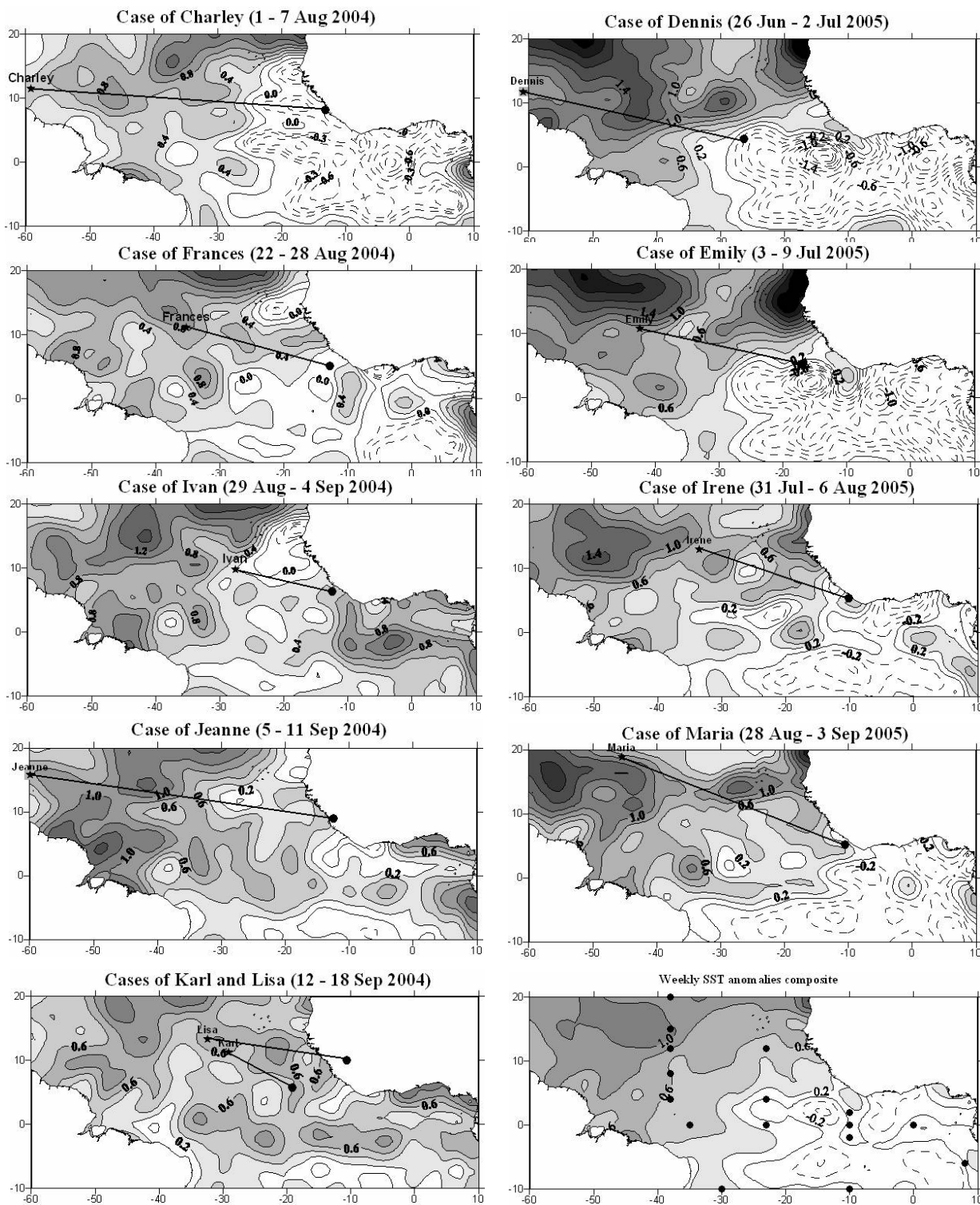


Figure 8: Weekly SST anomalies averaged over each period ranged between MCS dissipations and H initiations during 2004 (left) and 2005 (right). Interval contour is 0.2°C . Coordinates of MCS dissipations and H initiations are marked as in Fig. 7. The right-bottom panel (with the schematically locations of the PIRATA array) represents the average of all the other panels.

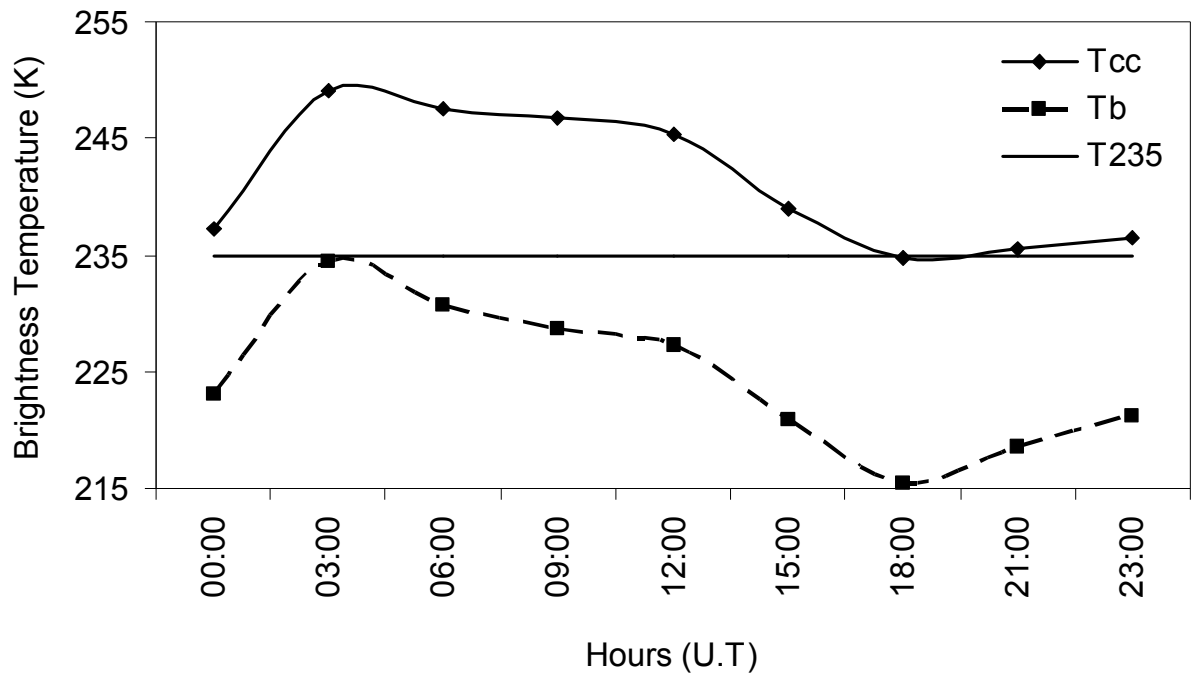


Figure A1: Threshold temperatures used to track the MCSs in the ocean. The continuous curve (Tcc) is the dynamical threshold temperature used to define the MCSs and the dotted curve (Tb) is the dynamical threshold temperature used to define the convective cells merged inside the MCSs. The fixed T_{235} is represented by a horizontal line.

Table 1: Summary information on the ten cases selected in 2004 and 2005 when hurricanes were associated to MCSs originating from the African continent. Distance (km) and time lag (day) between MCS dissipations and hurricane initiations are indicated, as well as the mean virtual velocity (m s^{-1}). MCS initiation dates and their lifespan are also given.

Hurricane initiations			MCS dissipations		Calculated lags			MCS initiations	
Name	Date	coordinates	Date	Coordinates	Distance (km)	Time (day)	Virtual velocity (m s^{-1})	Date	Lifespan (hour)
Charley	08/09/04	11.4°N;	08/03/04	8.11°N ;	4616	5.7	9.5	08/02/04	25.5
	12:00 UT	59.2°W	20:30 UT	13.16°W				19:00 UT	
Frances	08/25/04	11.1°N;	08/21/04	5.10°N;	2317	3.1	8.6	08/20/04	28
	00:00 UT	35.2°W	21:00 UT	12.82°W				17:00 UT	
Ivan	09/02/04	9.7°N;	08/31/04	6.34°N;	1545	1.9	9.3	08/30/04	25
	18:00 UT	27.6°W	19:00 UT	12.52°W				18:00 UT	
Jeanne	09/13/04	15.9°N;	09/07/04	9°N;	4804	5.7	9.8	09/06/04	22.5
	18:00 UT	60°W	14:30 UT	12.46°W				16:00 UT	
Karl	09/16/04	11.2°N;	09/15/04	5.75°N;	1147	1.2	11.5	09/13/2004	37.5
	06:00 UT	29.2°W	02:30 UT	19.11°W				13:00 UT	
Lisa	09/19/04	13.3°N;	09/16/04	10.03°N;	2205	2.8	9.2	09/14/04	43.5
	18:00 UT	32.4°W	11:30 UT	10.59°W				16:00 UT	
Dennis	07/04/05	12°N;	06/30/05	4.44°N;	3532	4.0	10.2	06/26/05	87.5
	18:00 UT	60.8°W	05:30 UT	26.30°W				14:00 UT	
Emily	07/11/05	10.7°N;	07/07/05	5.25°N;	2594	3.7	8.1	07/05/2005	44
	00:00 UT	42.4°W	07:00 UT	17.04°W				11:00 UT	
Irene	08/04/05	12.9°N;	08/02/05	5.35°N ;	2452	2.6	11.1	07/31/05	36.5
	18:00 UT	33.5°W	04:30 UT	10.17°W				16:00 UT	
Maria	09/01/05	18.8°N;	08/27/05	5.26°N;	3752	4.7	9.3	08/26/05	31.5
	12:00 UT	45.5°W	19:30 UT	10.51°W				12:00 UT	
Average					2896	3.5	9.7 ± 1.0		

Table A1: Summary information on the tracking MCSs for the case of August 2004 between 44°W – 20°E; 25°S – 25°N.

	T235	Tcc	Tcc / T235
Total MCS number	356251	474624	1.3
Cloud cover per image (km ²)	2110555	3024479	1.4
lifespan (hour)		MCS cycles	
[0.5 ; 10[9539	11954	1.3
[10 ; 40[578	628	1.1
[40 ; 80[32	35	1.1
[80 ; 100[1	2	2.0
Total number of MCS cycles	10150	12619	1.2